JACS
JOURNAL OF THE AMERICAN CHEMICAL SOCIETY

Article

pubs.acs.org/JACS

Smart Mesoporous SiO_2 Nanoparticles for the DNAzyme-Induced Multiplexed Release of Substrates

Zhanxia Zhang, Dora Balogh, Fuan Wang, and Itamar Willner*

Institute of Chemistry, The Center for Nanoscience and Nanotechnology, The Hebrew University of Jerusalem, Jerusalem 91904, Israel

Supporting Information

ABSTRACT: The fluorescent dyes methylene blue, MB^+, and thionine, Th^+, can be trapped in the pores of mesoporous silica, MP-SiO_2, by means of functional nanostructures consisting of the Mg^{2+}- or Zn^{2+}-dependent DNAzyme sequences. In the presence of Mg^{2+} or Zn^{2+} ions the respective DNAzymes are activated, leading to the specific cleavage of the respective caps, and the selective release of MB^+ or Th^+. The enlargement of the conserved loop domains of the Mg^{2+}- or Zn^{2+}-dependent DNAzyme sequences with foreign nucleotides prohibits the formation of active DNAzymes and eliminates the release of the respective dyes. This is due to the flexibility of the loops that lacks affinity for the association of the ions. The insertion of aptamer sequences (e.g., the adenosine-5′-triphosphate (ATP) aptamer) or ion-binding sequences (e.g., T-rich Hg^{2+} ion-binding domains) as foreign components to the loop regions allows the formation of active Mg^{2+}- or Zn^{2+}-dependent DNAzyme structures through the cooperative formation of aptamer-ATP complexes or T-Hg^{2+}-T bridges. These aptamer−substrate complexes or T-Hg^{2+}-T bridges allosterically stabilize and activate the DNAzymes, thus allowing the selective release of the fluorescent substrates MB^+ or Th^+. The metal ion-driven DNAzyme release of substrates from the pores of MP-SiO_2, and particularly the allosteric activation of the DNAzymes through cooperative aptamer−substrate complexes or metal-ion bridges, has important future nanomedical implications for targeted release of drugs. This is demonstrated with the triggered release of the anticancer drug, doxorubicin, by the Mg^{2+}-DNAzyme-locked pores or by the aptamer-ATP complex-triggered activation of the Mg^{2+}-dependent DNAzyme.

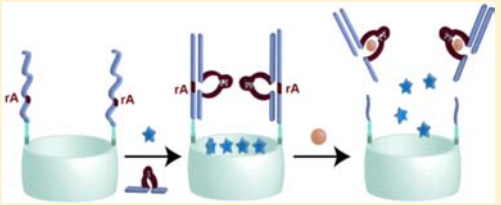

INTRODUCTION

Mesoporous silica (MP-SiO_2) attracts substantial research interests due to its porous structure that allows the encapsulation of substrates in the pores and due to the ability to chemically modify its surface. These properties were applied to use MP-SiO_2 as a versatile hybrid material for catalysis,[1−3] drug delivery,[4−6] and imaging.[7−9] Furthermore, chemical modification of MP-SiO_2 enables the design of signal-responsive matrices for the controlled release of substrates from their pores. Different stimuli such as pH,[10−12] photonic signals,[13,14] redox reagents,[15−17] or enzymes[18−21] were implemented to trigger the opening of the pores, leading to the controlled release of encapsulated substrates. Accordingly, the pores of the MP-SiO_2 were capped with gate units that locked the substrate in the pores and allowed the stimuli-responsive unlocking of the gates and the release of the substrates. For example, the photonic dethreading of semi-rotaxane pore-capping nanostructures was implemented to open the pores and release the stored substrate.[22,23]

The information encoded in the base sequences of nucleic acids provides a rich arena of opportunities to develop the area of DNA nanotechnology.[24−26] Sequence-guided and pH-stimulated assembly of single-stranded DNA into i-motif structures[27−29] or the cooperative binding of DNA duplexes by metal ions, e.g., by T-Hg^{2+}-T bridges, were implemented to construct different DNA machines,[30−32] and to develop logic gates[33,34] and finite state logic machines.[35] Similarly, sequence-specific nucleic acid strands reveal specific binding properties toward low-molecular-weight or macromolecular substrates (aptamers),[36−38] or exhibit catalytic properties (DNAzymes).[39−42] Indeed, the aptamers have been implemented to develop DNA machines[43,44] to assemble programmed nanostructures,[45−47] and DNA nanostructures were implemented for the stimuli-controlled transport through nanochannels.[48,49] Catalytic nucleic acids were used to develop logic gates and logic gate cascades.[50−52] Not surprisingly, the conjugation of nucleic acids to MP-SiO_2 enabled the implementation of the signal-triggered functions of the DNA to "lock" and "unlock" the pores of the MP-SiO_2. For example, the pores were loaded with a dye substrate and "locked" by i-motif, C-quadruplex capping units, and subsequently "unlocked" by the separation of the bulky i-motif structure to random single strands, at neutral pH values, thus allowing the release of the substrates.[53] In a related system the change of the pH and the opening of the pores was stimulated by a photochemical process.[54] Alternatively, the pores of the MP-SiO_2 were capped with duplex DNA units, and the capping strands were separated by a strand displacement process, in the presence of Hg^{2+} ions, to yield a T-Hg^{2+}-T bridged duplex structure of enhanced stability. The

Received: November 22, 2012
Published: January 8, 2013

   dx.doi.org/10.1021/ja311385y | J. Am. Chem. Soc. 2013, 135, 1934−1940

release of the pore-entrapped substrate enabled the fluorescence detection of Hg^{2+} ions.[55] In the present study, we introduce metal-dependent catalytic nucleic acids as functional triggers for opening the pores of the MP-SiO_2 and releasing the pore-entrapped fluorescent substrates. Combination of two kinds of MP-SiO_2 hybrids that are functionalized with the Mg^{2+}- and Zn^{2+}-dependent DNAzymes[56−58] as capping units that lock two different fluorophores in the pores effects the selective (or multiplexed) release of a fluorophore by the respective ion. In addition, we demonstrate that composite DNA structures consisting of enlarged loops of the Mg^{2+}- and Zn^{2+}-DNAzyme sequences block the dyes (entrapped substrates) in two kinds of pores of the mesoporous materials even in the presence of the Mg^{2+} or Zn^{2+} ions. The opening of the pores by the respective DNAzyme proceeds only upon the cooperative formation of an aptamer−substrate complex or metal ion−nucleic acid bridge, a process that triggers the formation of the active DNAzyme structure. Since the pores are opened in the presence of the specific ions (Mg^{2+}, Zn^{2+}) or upon the cooperative incorporation of aptamer−substrate (adenosine-5′-triphosphate [ATP]) or coadded metal ions (Hg^{2+}), one may consider these added components as inputs for logic operations, and the triggered opening of the pores and the release of the entrapped substrates as outputs for these logic operations. The relevance of these programmed mesoporous release systems for future nanomedicine is discussed. The unique and innovative facets of the study rest on the fact that the metal ion-dependent catalytic nucleic acids (DNAzymes) are synthetic sequences, where the loop domain in these sequences binds a specific ion to yield catalytic functions. As a result, the opening of the pores, protected by a sequence-specific DNAzyme nanostructure, proceeds selectively by the specific metal ion, acting as cofactor for the DNAzyme sequence.

RESULTS AND DISCUSSION

MP-SiO_2 nanoparticles (NPs) (350−400 nm in diameter, see Figure S1, Supporting Information [SI]) were prepared according to the literature.[53] The pore diameter was estimated to be 3 nm, the surface area of the mesoporous composite corresponded to 632.8 m^2/g, and the average pore volume corresponded to 7.2×10^{-2} cm^3/g. The NPs were functionalized with the thiolated ribonucleo-base-containing sequence (**1**) according to Figure 1A. (**1**) corresponds to the sequence of the substrate of the Mg^{2+}-dependent DNAzyme,[56,57] and to the substrate of the Zn^{2+}-dependent DNAzyme.[58] The (**1**)-functionalized MP-SiO_2 was interacted with methylene blue, MB^+, (**2**), as guest substrate, or was subjected to a solution of thionine, Th^+, (**3**), to load the mesoporous NPs, respectively. The MB^+-loaded MP-SiO_2 and the Th^+-loaded MP-SiO_2 were then treated with the respective Mg^{2+}- or Zn^{2+}-dependent DNAzyme sequences (**4**) or (**5**). The hybridization of the DNAzyme sequences (**4**) and (**5**) with the (**1**)-functionalized particles yielded duplex structures that trapped the dyes MB^+ or Th^+ in the pores of the MP-SiO_2. The resulting SiO_2 NPs were extensively washed to remove any MB^+ or Th^+ units associated with surface domains outside the pores (see Figure S2, SI). The resulting NPs retained dark colors of nondissociable dyes, implying that the dyes are, indeed, entrapped in the MP-SiO_2 pores in locked configurations. Figure 1B depicts the principle of the ion-mediated, selective, release of the MB^+ or Th^+ dyes from the respective MP-SiO_2 container matrices. In the presence of either Mg^{2+} or Zn^{2+} ions, the active Mg^{2+}- or

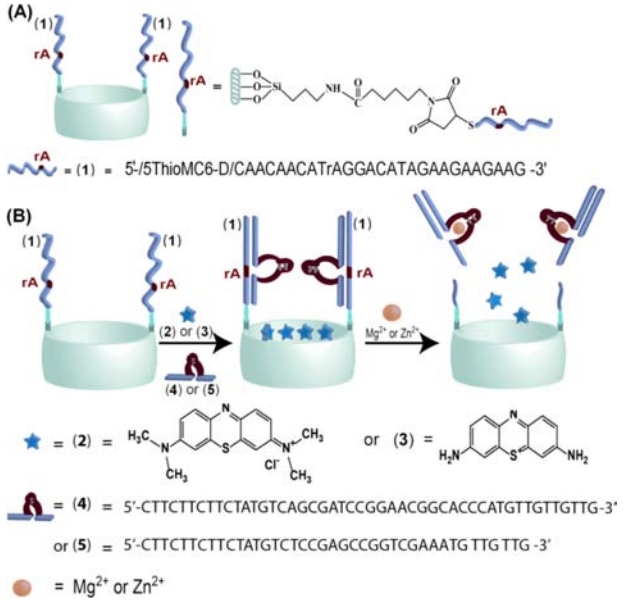

Figure 1. (A) Schematic presentation of the SiO_2 nanopores functionalized with the thiolated sequence (**1**), using *N*-ε-maleimidocaproyl-oxysulfosuccinimide ester (sulfo-EMCS) as a cross-linker. (B) Schematic presentation of the ion-mediated release of MB^+ or Th^+ from the nanocontainers, using the Mg^{2+}-dependent or Zn^{2+}-dependent DNAzyme, respectively.

Zn^{2+}-dependent DNAzymes are generated on the (**1**)/(**4**)-functionalized MP-SiO_2 or (**1**)/(**5**)-functionalized MP-SiO_2, respectively. This results in the cleavage of the substrates (**1**), leading to the dissociation of the duplex DNA-caps and the release of MB^+ or Th^+, respectively. Figure 2A shows the fluorescence of MB^+ observed in the bulk solution after a fixed time-interval of 60 min upon treatment of the (**1**)/(**4**)-functionalized MP-SiO_2 with different concentrations of Mg^{2+}. As the concentration of Mg^{2+} increases, the fluorescence of MB^+, generated in the bulk solution, through the release from the pores, is intensified. Figure 2B depicts the resulting calibration curve, indicating that at a Mg^{2+} concentration of ca. 10 mM the release of MB^+ from the pores reaches a saturation value. Figure 2C, curve (a), shows the time-dependent fluorescence changes upon treatment of the (**1**)/(**4**)-functionalized MP-SiO_2 with Mg^{2+} ions (10 mM). The fluorescence in the bulk solution increases with time and reaches a saturation value after ca. 60 min. For comparison, Figure 2C, curve (b), depicts the time-dependent fluorescence changes in the solution upon treatment of the (**1**)/(**4**)-modified MP-SiO_2 in the absence of Mg^{2+}. The fluorescence changes are substantially lower, and these may be attributed to desorption of residual from surface domains at the exterior of the pores, or to the slow leakage of MB^+ from the incompletely blocked pores. From the fluorescence intensity obtained in the (**1**)/(**4**)-MP-SiO_2 system after 60 min of release of MB^+, and using an appropriate calibration curve, we estimate that ca. 2.7 μmol of MB^+/g SiO_2 NPs were released by the DNAzyme-mediated cleavage of the capping units. Figure 2D shows the time-dependent fluorescence changes upon treatment the (**1**)/(**4**)-modified MP-SiO_2 NPs with different metal ions. Clearly, selectivity is demonstrated, and only in the presence of Mg^{2+}, enhanced fluorescence in the bulk solution can be observed, as a result of the release of MB^+ from the pores. These results indicate that the Mg^{2+}-dependent DNAzyme cleaves off the duplex-DNA-

dx.doi.org/10.1021/ja311385y | J. Am. Chem. Soc. 2013, 135, 1934−1940

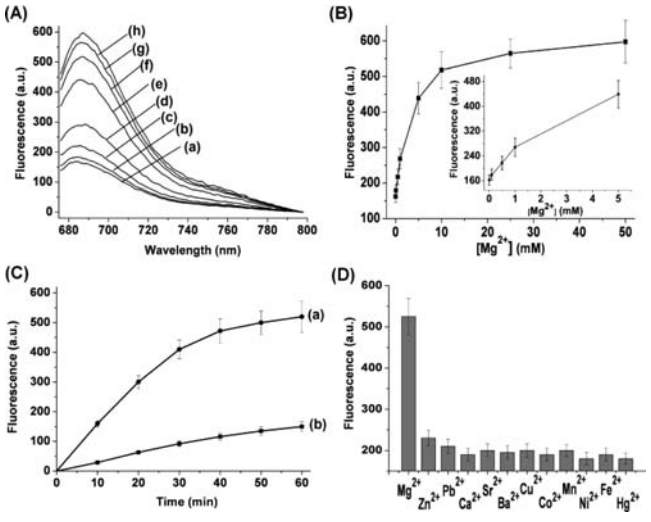

Figure 2. (A) Fluorescence spectra of MB^+ in the solution upon addition of variable concentrations of Mg^{2+} ions to the MB^+-loaded SiO_2 NPs: (a) 0 mM, (b) 0.1 mM, (c) 0.5 mM, (d) 1 mM, (e) 5 mM, (f) 10 mM, (g) 25 mM, (h) 50 mM; followed by the release of MB^+ to the solution for a fixed time-interval of 60 min. (B) Calibration curve corresponding to the fluorescence changes upon release of MB^+ from the pores of the (**1**)/(**4**)-functionalized SiO_2 NPs as a function of the Mg^{2+} ion concentration. (C) Time-dependent fluorescence changes upon the release of MB^+. (a) Upon the treatment of the (**1**)/(**4**)-functionalized SiO_2 NPs with 10 mM Mg^{2+} ions and (b) upon the treatment of the (**1**)/(**4**)-functionalized SiO_2 NPs in the absence of Mg^{2+} ions. (D) Fluorescence changes of MB^+ upon the treatment of the (**1**)/(**4**)-functionalized SiO_2 NPs with different metal ions (10 mM) for a time-interval of 60 min.

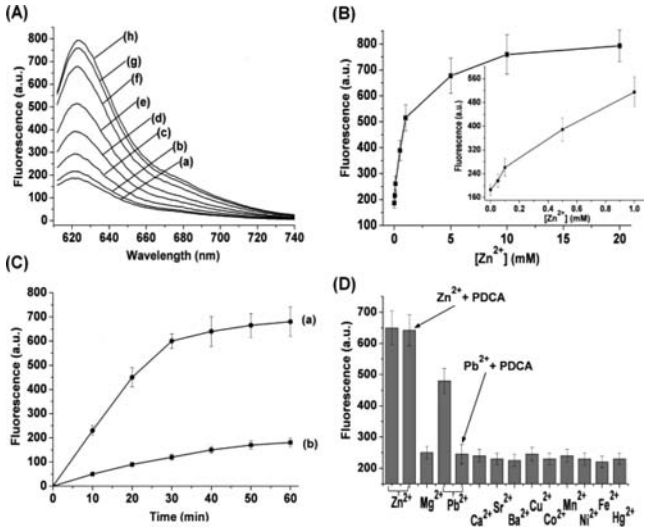

Figure 3. (A) Fluorescence spectra of Th^+ in the solution upon the addition of variable concentrations of Zn^{2+} ions to the Th^+-loaded SiO_2 NPs: (a) 0 mM, (b) 0.05 mM, (c) 0.1 mM, (d) 0.5 mM, (e) 1 mM, (f) 5 mM, (g) 10 mM, (h) 20 mM. The release of Th^+ into the solution is monitored after a fixed time interval of 40 min. (B) Calibration curve corresponding to the fluorescence changes upon release of Th^+ from the pores of the (**1**)/(**5**)-functionalized SiO_2 NPs as a function of the Zn^{2+} ions concentration. (C) Time-dependent fluorescence changes upon the release of Th^+: (a) Upon the treatment of the (**1**)/(**5**)-functionalized SiO_2 NPs with 5 mM Zn^{2+} ions. (b) Upon the treatment of the (**1**)/(**5**)-functionalized SiO_2 NPs in the absence of Zn^{2+} ions. (D) Fluorescence changes of Th^+ upon the treatment of the (**1**)/(**5**)-functionalized SiO_2 NPs with different metal ions (5 mM) for a fixed time interval of 40 min. (The concentration of PDCA for the elimination of the Pb^{2+} interference was 10 mM.)

locking units, thus enabling the release of MB^+ from the pores. Particularly interesting is the demonstrated selectivity, showing that the (**1**)/(**4**)-modified MP-SiO_2 composite is insensitive to Zn^{2+}. This allows the selective activation of the (**1**)/(**5**)-modified MP-SiO_2 by Zn^{2+} ions and the release of thionine from this composite.

Similar results were demonstrated with the (**1**)/(**5**)-functionalized entrapped thionine, (**3**). Figure 3A depicts the fluorescence intensities of Th^+ in the bulk solution, upon treatment of the (**1**)/(**5**)-functionalized MP-SiO_2 NPs with different concentrations of Zn^{2+} ions, for a fixed time-interval of 40 min. As the concentration of Zn^{2+} increases, the fluorescence in the bulk solution is intensified, consistent with the enhanced release of Th^+ from the pores. The resulting calibration curve is shown in Figure 3B, indicating that the fluorescence levels off to a saturation value at a Zn^{2+} concentration of ~5 mM. Figure 3C, curve (a) shows the time-dependent fluorescence changes upon treatment of the (**1**)/(**5**)-functionalized MP-SiO_2 in the presence of Zn^{2+}, 5 mM, while curve (b) depicts the time-dependent fluorescence changes in the absence of the Zn^{2+} ions. Evidently, the time-dependent fluorescence changes that cumulate with the amount of released Th^+, are substantially higher in the presence of the activated Zn^{2+}-dependent DNAzyme after a fixed time interval of 40 min. From the fluorescence intensity obtained and using the appropriate calibration curve we estimate that ~3.9 μmol of Th^+/g SiO_2 NPs were released from the pores. The time-dependent fluorescence changes in the absence of Zn^{2+} ions are attributed to the leakage of Th^+ from the pores due to incomplete blocking of the pores by the (**1**)/(**5**) duplexes and/or to residual Th^+ desorbed from nonpore domains on the NPs.

The enhanced release of Th^+ from the pores proceeds only in the presence of Zn^{2+} ions, and all other added ions (except Pb^{2+}) do not affect the release of Th^+ from the pores, Figure 3D. The interference of Pb^{2+} to the selective opening of the pores can be eliminated by the addition of 2,6-pyridine-dicarboxylic acid (PDCA), that act as a selective ligand for binding Pb^{2+} ions. We find that in the presence of PDCA the Pb^{2+}-induced opening of the pores is eliminated, while the Zn^{2+} ion-stimulated opening of the pores is unaffected. Thus, we conclude that the Zn^{2+}-dependent DNAzyme activates only the release of Th^+ from the (**1**)/(**5**)- functionalized MP-SiO_2 containers. As expected, the treatment of the mixture consisting of the MB^+-loaded (**1**)/(**4**)-modified MP-SiO_2 NPs, and of the Th^+-loaded (**1**)/(**5**)-functionalized MP-SiO_2 NPs with Mg^{2+} and Zn^{2+} ions resulted in the release of MB^+ and Th^+ from the two kinds of nanoparticle containers. Accordingly, the Mg^{2+} and Zn^{2+} ions may be considered as inputs for the activation of an "AND" logic gate operation, Figure 4. A dual fluorescence output of MB^+ and Th^+ is considered as a "true" output, "1". Thus, in the absence of the inputs (0,0) only very low fluorescence is observed, output "0", Figure 4A. In the presence of Mg^{2+} or Zn^{2+}, inputs (1,0) or (0,1), only one intense fluorescence output of MB^+ or Th^+ is generated (metal ion-output "0"), Figure 4B and C. In the presence of Mg^{2+} and Zn^{2+} ions, intense fluorescence bands of the two dyes MB^+ and Th^+ are observed, giving rise to an output "1", Figure 4D, "AND" gate.

The activities of metal ion-dependent DNAzymes are controlled by conserved base sequences in the hairpin loops

dx.doi.org/10.1021/ja311385y | J. Am. Chem. Soc. 2013, 135, 1934−1940

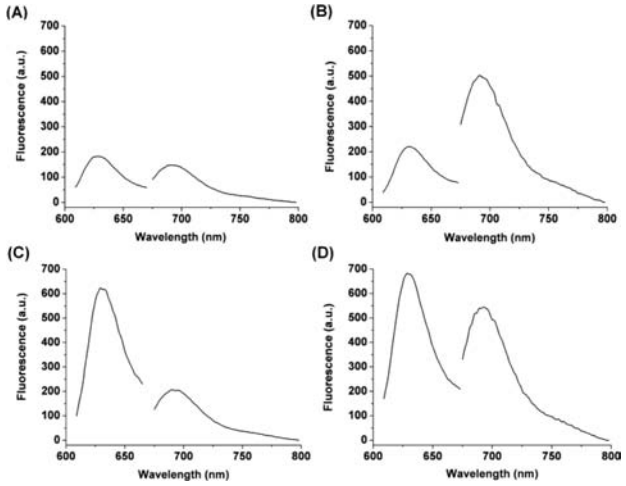

Figure 4. Dual fluorescence outputs of MB^+ and Th^+ in the presence of Mg^{2+} and Zn^{2+} as inputs: (A) in the absence of the inputs, (0,0); (B) in the presence of Mg^{2+} (10 mM) and Zn^{2+} (0 mM), (1,0); (C) in the presence of Mg^{2+} (0 mM) and Zn^{2+} (5 mM), (0,1); and (D) in the presence of Mg^{2+} (10 mM) and Zn^{2+} (5 mM), (1,1). The ratio of the Th^+- and MB^+-loaded mesoporous SiO_2 NPs is 1:1.

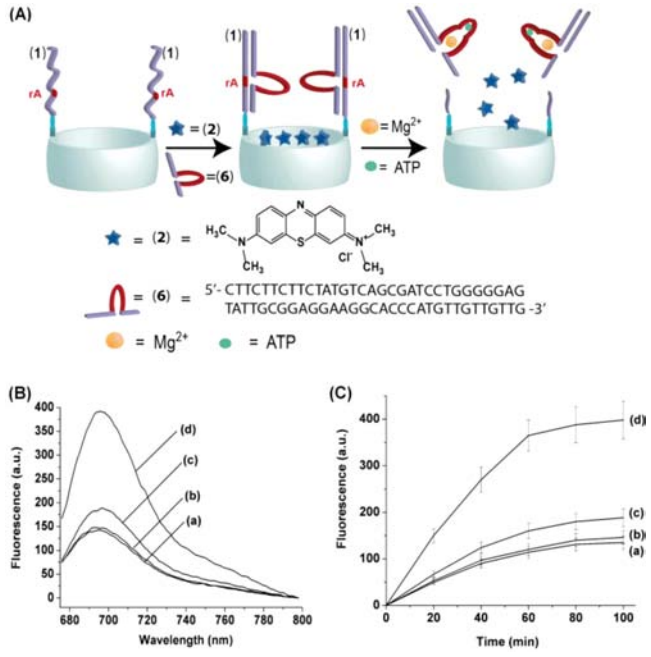

Figure 5. (A) Schematic presentation of the ATP-aptamer complex-assisted ion-mediated release of MB^+ from the nanocontainers. (B) Fluorescence spectra of MB^+ in the solution upon the addition of (a) 0 Mg^{2+}, 0 ATP; (b) 0 Mg^{2+}, 100 μM ATP; (c) 20 mM Mg^{2+}, 0 ATP; (d) 20 mM Mg^{2+}, 100 μM ATP, after a fixed time interval of 90 min. (C) Time-dependent fluorescence changes upon the release of MB^+ using (a) 0 Mg^{2+}, 0 ATP; (b) 0 Mg^{2+}, 100 μM ATP; (c) 20 mM Mg^{2+}, 0 ATP; (d) 20 mM Mg^{2+}, 100 μM ATP.

that bind the respective metal ions, and by conserved sequences for the binding of the DNAzyme substrates. Previous studies demonstrated that the incorporation of foreign bases into the sequence-specific loops of DNAzymes perturb the binding affinity of the loops toward the metal ions, presumably due to the flexibility of the added base chains, leading to a decrease in the DNAzyme activities. Thus, the incorporation of flexible foreign oligonucleotide sequences into the Mg^{2+}- or Zn^{2+}-sequence-specific loops is anticipated to perturb the DNAzyme activities. The programming of these added foreign sequences, to bind auxiliary substrates/metal ions (e.g., by the formation of loops or duplexes) could, however, rigidify the loop sequences of the DNAzymes, thus restoring the biocatalytic activities. That is, by the programming of aptamer sequences or interchain metal-binding sequences into the DNAzyme loops the allosteric activation of the DNAzymes through the formation of aptamer−substrate complexes or metal ion-stabilized duplexes may be envisaged. This paradigm was implemented to effect the release of MB^+ from the MB^+-loaded MP-SiO_2 through the ATP-aptamer complex-aided or through the thymine-Hg^{2+}-thymine-assisted activation of the Mg^{2+}-dependent DNAzyme. Figure 5A shows schematically the nucleic acid nanostructure that leads to the ATP-guided assembly of the Mg^{2+}-dependent DNAzyme, resulting in the release of MB^+ from the pores. The nucleic acid (**6**) includes the base sequence characteristic to the Mg^{2+}-dependent DNAzyme and an inserted sequence comprising of the ATP aptamer sequence. The hybridization of (**6**) and the (**1**)-functionalized MP-SiO_2 is anticipated to form a flexible loop structure, revealing low affinity for the binding of Mg^{2+}, thus, leading to an inefficient catalyst for cleaving (**1**), and releasing the pore-entrapped MB^+. In the presence of ATP, the aptamer domain is expected to fold into a hairpin aptamer-ATP complex, thus leading to the rigidification of the DNAzyme sequence and to the spatial proximity of the bases associated with the DNAzyme sequence. Under these conditions, we expect that effective binding of Mg^{2+} to the DNAzyme loop will proceed. This will activate the DNAzyme to cleave (**1**), while releasing MB^+ from the pores. Accordingly, MB^+ was entrapped in the pores of the (**1**)-modified MP-SiO_2 NPs through the hybridization of (**6**) with (**1**), using the (**1**)/(**6**) nanostructures as stopper units for the pores. Figure 5B, curve (a), shows the fluorescence spectra of MB^+ in the bulk solution upon stirring the (**1**)/(**6**)-modified, MB^+-locked MP-SiO_2 NPs, for 90 min, in an aqueous solution. A low fluorescence band of MB^+ is observed, that is attributed to the leakage of MB^+ from the pores and the partial desorption of traces of MB^+ associated with nonpore domains. Figure 5B, curve (b), depicts the fluorescence intensity generated by the system in the presence of added ATP. No effect of ATP on the resulting fluorescence is observed, implying that ATP alone has no effect on the opening of the pores. In the presence of Mg^{2+}, but without added ATP, the fluorescence generated by the system increases by 38%, Figure 5B, curve (c). This value of fluorescence should be compared to the fluorescence generated under similar conditions by the (**1**)/(**4**)-functionalized MP-SiO_2 in the presence of Mg^{2+}, (cf. Figure 2C, curve (a) that reveals a 3.1-fold higher fluorescence). Thus, the results indicate that the mutated strand (**6**) that includes the inserted aptamer sequence exhibits low catalytic activity, presumably due to flexibility of the strand (**6**) that does not bind Mg^{2+} ions efficiently. In turn, the addition of ATP to the system, in the presence of Mg^{2+} ions results in the efficient release of the MB^{2+} from the pores and a high fluorescence, Figure 5B, curve (d), These results clearly imply that the formation of the ATP aptamer complex results in the assembly of a rigidified loop for binding Mg^{2+}, leading to an effective catalyst for the cleavage of (**1**) and the opening of the pores. Figure 5C shows the time-dependent fluorescence changes in the different systems. From the saturated fluorescence value generated by the ATP aptamer−(**1**)/(**6**)-

dx.doi.org/10.1021/ja311385y | J. Am. Chem. Soc. 2013, 135, 1934−1940

modified MB^+-loaded MP-SiO_2 system, and using an appropriate calibration curve, we estimated that, after a time interval of 90 min, ~1.9 μmol of MB^+ /g SiO_2 NPs were released from the pores. Very similar results are observed upon the insertion of the ATP aptamer sequence into the loop region of the Zn^{2+}-dependent DNAzyme, (see Figure S3, SI). We find that, while the Zn^{2+}-DNAzyme mutated sequence is inefficient in releasing thionine from the MP-SiO_2 pores, the allosteric formation of the ATP-aptamer complex assembles an active Zn^{2+}-DNAzyme loop that leads to the effective opening of the pores and the release of thionine.

The previous examples have demonstrated the allosteric activation of the Mg^{2+}-dependent DNAzyme and of the Zn^{2+}-dependent DNAzyme through the formation of aptamer–substrate complexes, thus leading to the triggered opening of the pores of the MP-SiO_2 and to the effective release of MB^+ or Th^+ from the pores. A similar allosteric control of DNAzyme activity was achieved by using metal ions (e.g., Hg^{2+}) as promoters. This is exemplified in Figure 6A, where the nucleic

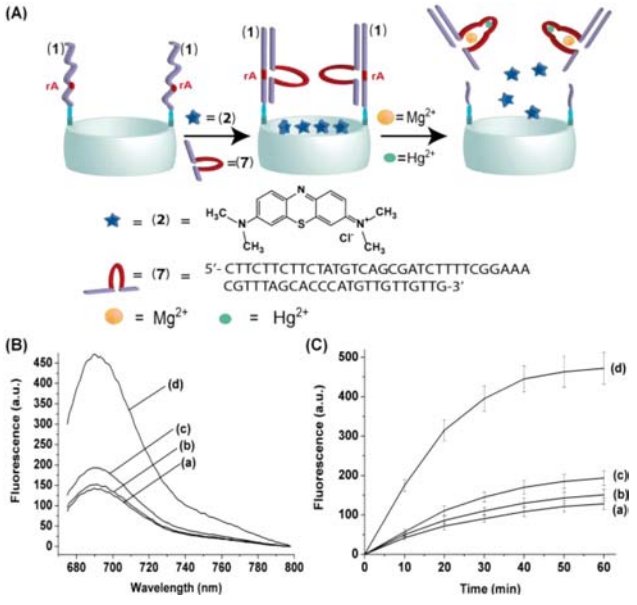

Figure 6. (A) Schematic presentation of the Hg^{2+}-assisted Mg^{2+}-dependent DNAzyme-mediated release of MB^+ from the nanocontainers. (B) Fluorescence spectra of MB^+ in the solution upon the addition of (a) 0 Mg^{2+}, 0 Hg^{2+}; (b) 0 Mg^{2+}, 1 μM Hg^{2+}; (c) 20 mM Mg^{2+}, 0 Hg^{2+}; (d) 20 mM Mg^{2+}, 1 μM Hg^{2+}, after a time interval of 60 min. (C) Time-dependent fluorescence changes upon the release of MB^+ using (a) 0 Mg^{2+}, 0 Hg^{2+}; (b) 0 Mg^{2+}, 1 μM Hg^{2+}; (c) 20 mM Mg^{2+}, 0 Hg^{2+}; (d) 20 mM Mg^{2+}, 1 μM Hg^{2+}.

acid (**7**) consists of two domains of the Mg^{2+}-dependent DNAzyme, where a foreign sequence that includes 6 thymine bases is inserted into the conserved DNAzyme sequence. The T-rich domain is capable of forming, in the presence of Hg^{2+} ions, a T-Hg^{2+}-T bridged hairpin structure. Thus, the hybridization of (**7**) with the (**1**)-functionalized MP-SiO_2 results in the locking of MB^+ in the pores of the matrix. The enlarged loop structure of (**7**), along with its flexibility, is anticipated to yield a poor nanoenvironment for the binding of Mg^{2+}, and thus an inefficient DNAzyme for "unlocking" the pores is formed. In the presence of Hg^{2+} ions, the inserted sequence forms a T-Hg^{2+}-T hairpin bridged structure, and this contacts and rigidifies the DNAzyme loop structure. As a result, the added Hg^{2+} allosterically activates the Mg^{2+}-DNAzyme structure, thus allowing the catalytic cleavage of (**1**), the opening of the pores, and the release of the pore-loaded MB^+. Figure 6B depicts the fluorescence spectra of the bulk solution upon interaction of the (**1**)/(**7**)-locked MB^+–MP-SiO_2 in the absence of Mg^{2+} ions and Hg^{2+} ions, curve (a), or only in the presence of Hg^{2+} ions, curve (b). Only a residual, low-intensity fluorescence is detected that is identical in the absence or presence of Hg^{2+} ions. These results indicate that the Hg^{2+} ions that interact with (**7**) do not promote the release of MB^+ from the pores. Treatment of the (**1**)/(**7**)–MB^+-loaded MP-SiO_2 with Mg^{2+} ions in the absence of Hg^{2+}, results in a very low increase in the fluorescence of the bulk solution, Figure 6B, curve (c), implying that the pores are still locked, resulting in the poor release of MB^+. In the presence of coadded Hg^{2+} ions and of Mg^{2+} ions, a high fluorescence is generated in the bulk solution, indicating the effective release of MB^+ from the pores (curve d). The time-dependent fluorescence changes upon releasing MB^+ from the different systems are depicted in Figure 6C. Thus, the coadded Hg^{2+} ions act as an allosteric promoter for the Mg^{2+}-dependent DNAzyme that catalyzes the cleavage of (**1**) and the release of (**2**) from the system. From the saturation level of the fluorescence generated by the Hg^{2+}/Mg^{2+}–(**1**)/(**7**) MB^+-loaded MP-SiO_2, Figure 6C, curve (d), and using the respective calibration curve we estimated that ~2.3 μmol of (**2**)/g SiO_2 NPs were released from the pores after a time interval of ~60 min. It should be noted that the formation of T-Hg^{2+}-T bridges is specific for Hg^{2+}, and other ions do not bridge the loop domain. Indeed, no allosteric effect in the activation of the Mg^{2+}-dependent DNAzyme in the presence of Zn^{2+}, Pb^{2+}, Ca^{2+}, Sr^{2+}, Ba^{2+}, Cu^{2+}, Co^{2+}, Mn^{2+}, Ni^{2+}, or Fe^{2+} was observed.

The metal ion-controlled release of the substrates from the mesoporous SiO_2 nanopores, and particularly the aptamer-assisted release of the entrapped substrate, might have important implications for future nanomedicine and targeted release of drugs. Toward these potential applications, we examined as a model system the Mg^{2+}-induced release of the anticancer drug doxorubicin. Figure 7A shows that the addition of Mg^{2+} ions to the (**1**)/(**4**)-capped doxorubicin-entrapped MP-SiO_2 pores leads to the opening of the pores and the release of the drug. Particularly interesting is the ATP-cooperative synergetic Mg^{2+}-opening of the pores and the release of doxorubicin. The rapid metabolism observed in cancer cells generates extensive amounts of ATP, and thus the

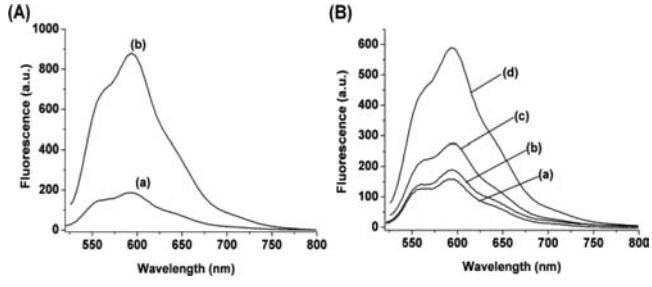

Figure 7. (A) Fluorescence spectra of doxorubicin in the solution after a time interval of 60 min, using the (**1**)/(**4**)-modified MP-SiO_2 NPs, in the absence (a) or in the presence (b) of 10 mM Mg^{2+} ions. (B) Fluorescence spectra of doxorubicin in the solution after a time interval of 90 min, using the (**1**)/(**6**)-modified MP-SiO_2 NPs, in the presence of (a) 0 Mg^{2+}, 0 ATP; (b) 0 Mg^{2+}, 100 μM ATP; (c) 20 mM Mg^{2+}, 0 ATP; (d) 20 mM Mg^{2+}, 100 μM ATP.

dx.doi.org/10.1021/ja311385y | J. Am. Chem. Soc. 2013, 135, 1934–1940

resulting ATP might act as an active unit for the targeted release of doxorubicin at cancer cells. Figure 7B shows that the doxorubicin entrapped in the pores by their capping with the (**1**)/(**6**) duplex structure is not released by ATP alone, is inefficiently released by only Mg^{2+} ions, yet is efficiently released by the addition of ATP and Mg^{2+} ions. That is, the binding of the ATP to the aptamer sequence of (**6**) rigidifies the loop sequence of the Mg^{2+}-dependent DNAzyme, thus leading to the effective cleavage of (**1**) and the opening of the pores.

CONCLUSIONS

The study has introduced the use of tailored nucleic acid nanostructures associated with mesoporous SiO_2 nanoparticles as functional units for the "locking" and "unlocking" of the pores. The nucleic acid gated nanostructures consisted of complex units composed of the metal-dependent catalytic nucleic acids and their substrates. While in the absence of the ions the complex structures "lock" the pores, in the presence of the respective ions, the catalytic functions of the nucleic acid are triggered "on", leading to the cleavage of the complex nucleic acids structures and to the "unlocking" of the pores. This results in the release of the pore-encapsulated substrates. The nucleic acid complex nanostructures that cap the pores consist of tailored sequences that selectively bind specific ions to their sequence-specific loop domains. As a result, the pores modified by different metal-dependent nucleic acid/substrate structures can be selectively unlocked by the ions specific for the respective DNAzyme sequences. The study has introduced several new concepts for the application of mesoporous SiO_2 NPs as nanocontainers for the controlled release of pore-entrapped substrates. (i) We introduced metal-dependent DNAzymes as functional components for "locking" and "unlocking" of the pores. The metal ion-driven catalytic properties of the DNAzymes provided the trigger to control the release of the pore-entrapped substrates. (ii) We have demonstrated the implementation of a mixture of two mesoporous SiO_2 matrices that were functionalized with Mg^{2+}- or Zn^{2+}-dependent DNAzymes as catalytic triggers for the multiplexed opening of the respective pores. One may envisage the use of other different metal-dependent DNAzymes. Furthermore, as different ion-dependent DNAzymes are operating at different pH values, one might program the DNAzyme-mediated opening of the pores by environmental pH changes. Such pH changes can also be modulated by electrochemical[59] or photochemical means.[54] (iii) We have demonstrated the selective metal ion-guided opening of the pores by the respective DNAzymes and the selective release of substrates from the pores. (iv) The ion-driven opening of the pores and the release of two different fluorescent dyes was rationalized in terms of a logic operation, where the ions act as inputs, and the released fluorophores, as readouts, providing the output signals. Thus, the systems may be considered as "smart materials" for the input-guided release of substrates. Such a system may be significant in future controlled drug delivery, targeted release of drugs, and signal-triggered release of promoters for the activation of prodrugs. (v) The allosteric activation of the DNAzymes associated with the MP-SiO_2 containers is of special interest and of immense potential impact. Our study has demonstrated the allosteric activation of the DNAzymes by aptamer−substrate complexes and the toxic Hg^{2+} ions. One may consider these systems as autonomous sense-and-treat systems that provide a new facet to future nanomedicine. The biomarker-guided formation of an aptamer complex or a toxic metal-stimulated activation of a DNAzyme could provide instructive sensing (recognition) events into the autonomous release of counteracting drugs. (vi) We have demonstrated the metal ion-guided and the aptamer/ATP−metal ion-stimulated release of the doxorubicin anticancer drug from the pores. The synergetic ATP-stimulated release of the doxorubicin is particularly interesting, as the system introduces a fundamental paradigm for future nanomedicine. The enhanced metabolic generation of ATP in cancer cells suggests that the opening of the pores and the release of doxorubicin might be targeted toward the cancer cells. Furthermore, the results imply that biomarkers or environmental conditions (e.g., pH) in cells might cooperatively activate DNAzymes and release drugs at specific targets. The cooperative activation of the DNAzymes by biomarker input(s) and the release of the encapsulated drug(s) may be considered as a logic gate operation, where the biomarkers provide the input(s), and the released substrate(s), the output(s).

ASSOCIATED CONTENT

Supporting Information

Supplementary figures and Experimental Section. This material is available free of charge via the Internet at http://pubs.acs.org.

AUTHOR INFORMATION

Corresponding Author

willnea@vms.huji.ac.il

Notes

The authors declare no competing financial interest.

ACKNOWLEDGMENTS

Parts of this study are supported by NanoSensoMach ERC Advanced Grant No. 267574 under the EC FP7/2007-2013 program and by the Volkswagen Foundation, Germany.

REFERENCES

(1) Jiao, F.; Frei, H. *Angew. Chem., Int. Ed.* **2009**, *48*, 1841−1844.
(2) Huh, S.; Chen, H.-T.; Wiench, J. W.; Pruski, M.; Lin, V. S.-Y. *Angew. Chem., Int. Ed.* **2005**, *44*, 1826−1830.
(3) Xiang, S.; Zhang, Y.; Xin, Q.; Li, C. *Chem. Commun.* **2002**, 2696−2697.
(4) Vallet-Regi, M.; Balas, F.; Arcos, D. *Angew. Chem., Int. Ed.* **2007**, *46*, 7548−7558.
(5) Zhao, Y.; Trewyn, B. G.; Slowing, I. I.; Lin, V. S.-Y. *J. Am. Chem. Soc.* **2009**, *131*, 8398−8400.
(6) Liong, M.; Lu, J.; Kovochich, M.; Xia, T.; Ruehm, S. G.; Nel, A. E.; Tamanoi, F.; Zink, J. I. *ACS Nano* **2008**, *2*, 889−896.
(7) Kim, J.; Kim, H. S.; Lee, N.; Kim, T.; Kim, H.; Yu, T.; Song, I. C.; Moon, W. K.; Hyeon, T. *Angew. Chem., Int. Ed.* **2008**, *47*, 8438−8441.
(8) Tsai, C.-P.; Hung, Y.; Chou, Y.-H.; Huang, D.-M.; Hsiao, J.-K.; Chang, C.; Chen, Y.-C.; Mou, C.-Y. *Small* **2008**, *4*, 186−191.
(9) Sakamoto, Y.; Kaneda, M.; Terasaki, O.; Zhao, D. Y.; Kim, J. M.; Stuckyk, G.; Shin, H. J.; Ryoo, R. *Nature* **2000**, *408*, 449−453.
(10) Yang, Q.; Wang, S.; Fan, P.; Wang, L.; Di, Y.; Lin, K.; Xiao, F.-S. *Chem. Mater.* **2005**, *17*, 5999−6003.
(11) Gao, Q.; Xu, Y.; Wu, D.; Shen, W.; Deng, F. *Langmuir* **2010**, *26*, 17133−17138.
(12) Zheng, H.; Wang, Y.; Che, S. *J. Phys. Chem. C* **2011**, *115*, 16803−16813.
(13) Liu, N.; Dunphy, D. R.; Atanassov, P.; Bunge, S. D.; Chen, Z.; Lopez, G. P.; Boyle, T. J.; Brinker, C. J. *Nano Lett.* **2004**, *4*, 551−554.
(14) Aznar, E.; Casasus, R.; Garcia-Acosta, B.; Marcos, M. D.; Martinez-Manez, R.; Sancenon, F.; Soto, J.; Amoros, P. *Adv. Mater.* **2007**, *19*, 2228−2231.

(15) Liu, R.; Zhao, X.; Wu, T.; Feng, P. *J. Am. Chem. Soc.* **2008**, *130*, 14418−14419.
(16) Luo, Z.; Cai, K.; Hu, Y.; Zhao, L.; Liu, P.; Duan, L.; Yang, W. *Angew. Chem., Int. Ed.* **2011**, *50*, 640−643.
(17) Wan, X.; Wang, D.; Liu, S. *Langmuir* **2010**, *26*, 15574−15579.
(18) Yu, A.; Wang, Y.; Barlow, E.; Caruso, F. *Adv. Mater.* **2005**, *17*, 1737−1741.
(19) Park, C.; Kim, H.; Kim, S.; Kim, C. *J. Am. Chem. Soc.* **2009**, *131*, 16614−16615.
(20) Lei, C.; Shin, Y.; Liu, J.; Ackerman, E. J. *J. Am. Chem. Soc.* **2002**, *124*, 11242−11243.
(21) Takahashi, H.; Li, B.; Sasaki, T.; Miyazaki, C.; Kajino, T.; Inagaki, S. *Chem. Mater.* **2000**, *12*, 3301−3305.
(22) Nguyen, T. D.; Tseng, H.-R.; Celestre, P. C.; Flood, A. H.; Liu, Y.; Stoddart, J. F.; Zink, J. I. *Proc. Natl. Acad. Sci. U.S.A.* **2005**, *102*, 10029−10034.
(23) Nguyen, T. D.; Liu, Y.; Saha, S.; Leung, K. C.-F.; Stoddart, J. F.; Zink, J. I. *J. Am. Chem. Soc.* **2007**, *129*, 626−634.
(24) Seeman, N. C. *Annu. Rev. Biophys. Biomol. Struct.* **1998**, *27*, 225−248.
(25) Yan, H.; Seeman, N. C. *J. Supramol. Chem.* **2001**, *1*, 229−237.
(26) Gao, H.; Kong, Y. *Annu. Rev. Mater. Res.* **2004**, *34*, 123−150.
(27) Choi, J.; Kim, S.; Tachikawa, T.; Fujitsuka, M.; Majima, T. *J. Am. Chem. Soc.* **2011**, *133*, 16146−16153.
(28) Sharma, J.; Chhabra, R.; Yan, H.; Liu, Y. *Chem. Commun.* **2007**, 477−479.
(29) Meng, H.; Yang, Y.; Chen, Y.; Zhou, Y.; Liu, Y.; Chen, X.; Ma, H.; Tang, Z.; Liu, D.; Jiang, L. *Chem. Commun.* **2009**, 2293−2295.
(30) Li, D.; Wieckowska, A.; Willner, I. *Angew. Chem., Int. Ed.* **2008**, *47*, 3927−3931.
(31) Miyake, Y.; Togashi, H.; Tashiro, M.; Yamaguchi, H.; Oda, S.; Kudo, M.; Tanaka, Y.; Kondo, Y.; Sawa, R.; Fujimoto, T.; Machinami, T.; Ono, A. *J. Am. Chem. Soc.* **2006**, *128*, 2172−2173.
(32) Ono, A.; Togashi, H. *Angew. Chem., Int. Ed.* **2004**, *43*, 4300−4302.
(33) Freeman, R.; Finder, T.; Willner, I. *Angew. Chem., Int. Ed.* **2009**, *48*, 7818−7821.
(34) Huang, W. T.; Shi, Y.; Xie, W. Y.; Luo, H. Q.; Li, N. B. *Chem. Commun.* **2011**, *47*, 7800−7802.
(35) Wang, Z.-G.; Elbaz, J.; Remacle, F.; Levine, R. D.; Willner, I. *Proc. Natl. Acad. Sci. U.S.A.* **2010**, *107*, 21996−22001.
(36) Liu, J.; Cao, Z.; Lu, Y. *Chem. Rev.* **2009**, *109*, 1948−1998.
(37) Tombelli, S.; Minunni, M.; Mascini, M. *Biosens. Bioelectron.* **2005**, *20*, 2424−2434.
(38) Willner, I.; Zayats, M. *Angew. Chem., Int. Ed.* **2007**, *46*, 6408−6418.
(39) Li, D.; Shlyahovsky, B.; Elbaz, J.; Willner, I. *J. Am. Chem. Soc.* **2007**, *129*, 5804−5805.
(40) Niazov, T.; Pavlov, V.; Xiao, Y.; Gill, R.; Willner, I. *Nano Lett.* **2004**, *4*, 1683−1687.
(41) Liu, J.; Lu, Y. *J. Am. Chem. Soc.* **2004**, *126*, 12298−12305.
(42) Liu, J.; Lu, Y. *J. Am. Chem. Soc.* **2007**, *129*, 9838−9839.
(43) Dittmer, W. U.; Reuter, A.; Simmel, F. C. *Angew. Chem., Int. Ed.* **2004**, *43*, 3550−3553.
(44) Shlyahovsky, B.; Li, D.; Weizmann, Y.; Nowarski, R.; Kotler, M.; Willner, I. *J. Am. Chem. Soc.* **2007**, *129*, 3814−3815.
(45) Liu, Y.; Lin, C.; Li, H.; Yan, H. *Angew. Chem., Int. Ed.* **2005**, *44*, 4333−4338.
(46) Kang, H.; O'Donoghue, M. B.; Liu, H.; Tan, W. *Chem. Commun.* **2010**, *46*, 249−251.
(47) Liu, J.; Lee, J. H.; Lu, Y. *Anal. Chem.* **2007**, *79*, 4120−4125.
(48) Hou, X.; Guo, W.; Xia, F.; Nie, F.-Q.; Dong, H.; Tian, Y.; Wen, L.; Wang, L.; Cao, L.; Yang, Y.; Xue, J.; Song, Y.; Wang, Y.; Liu, D.; Jiang, L. *J. Am. Chem. Soc.* **2009**, *131*, 7800−7805.
(49) Xia, F.; Guo, W.; Mao, Y.; Hou, X.; Xue, J.; Xia, H.; Wang, L.; Song, Y.; Ji, H.; Ouyang, Q.; Wang, Y.; Jiang, L. *J. Am. Chem. Soc.* **2008**, *130*, 8345−8350.
(50) Seelig, G.; Soloveichik, D.; Zhang, D. Y.; Winfree, E. *Science* **2006**, *314*, 1585−1588.
(51) Elbaz, J.; Lioubashevski, O.; Wang, F.; Remacle, F.; Levine, R. D.; Willner, I. *Nature Nanotechnol.* **2010**, *5*, 417−422.
(52) Winfree, E.; Qian, L. *Science* **2011**, *332*, 1196−1201.
(53) Chen, C.; Pu, F.; Huang, Z.; Liu, Z.; Ren, J.; Qu, X. *Nucleic Acids Res.* **2011**, *39*, 1638−1644.
(54) He, D.; He, X.; Wang, K.; Cao, J.; Zhao, Y. *Adv. Funct. Mater.* **2012**, *22*, 4704−4710.
(55) Zhang, Y.; Yuan, Q.; Chen, T.; Zhang, X.; Chen, Y.; Tan, W. *Anal. Chem.* **2012**, *84*, 1956−1962.
(56) Elbaz, J.; Shimron, S.; Willner, I. *Chem. Commun.* **2010**, *46*, 1209−1211.
(57) Wang, F.; Elbaz, J.; Teller, C.; Willner, I. *Angew. Chem., Int. Ed.* **2011**, *50*, 295−299.
(58) Li, J.; Zheng, W.; Kwon, A. H.; Lu, Y. *Nucleic Acids Res.* **2000**, *28*, 481−488.
(59) Frasconi, M.; Tel-Vered, R.; Elbaz, J.; Willner, I. *J. Am. Chem. Soc.* **2010**, *132*, 2029−2036.